JOURNAL OF BACTERIOLOGY, Nov. 1996, p. 6173–6183 Vol. 178, No. 21
0021-9193/96/$04.00+0

Structural Analysis of *Bacillus subtilis* 168 Endospore Peptidoglycan and Its Role during Differentiation

ABDELMADJID ATRIH,[1] PETER ZÖLLNER,[2] GÜNTER ALLMAIER,[2] AND SIMON J. FOSTER[1]*

Department of Molecular Biology and Biotechnology, University of Sheffield, Sheffield, S10 2TN, United Kingdom,[1] and Institute for Analytical Chemistry, University of Vienna, A-1090 Vienna, Austria[2]

Received 18 July 1996/Accepted 26 August 1996

The structure of the endospore cell wall peptidoglycan of *Bacillus subtilis* has been examined. Spore peptidoglycan was produced by the development of a method based on chemical permeabilization of the spore coats and enzymatic hydrolysis of the peptidoglycan. The resulting muropeptides which were >97% pure were analyzed by reverse-phase high-performance liquid chromatography, amino acid analysis, and mass spectrometry. This revealed that 49% of the muramic acid residues in the glycan backbone were present in the δ-lactam form which occurred predominantly every second muramic acid. The glycosidic bonds adjacent to the muramic acid δ-lactam residues were resistant to the action of muramidases. Of the muramic acid residues, 25.7 and 23.3% were substituted with a tetrapeptide and a single L-alanine, respectively. Only 2% of the muramic acids had tripeptide side chains and may constitute the primordial cell wall, the remainder of the peptidoglycan being spore cortex. The spore peptidoglycan is very loosely cross-linked at only 2.9% of the muramic acid residues, a figure approximately 11-fold less than that of the vegetative cell wall. The peptidoglycan from strain AA110 (*dacB*) had fivefold-greater cross-linking (14.4%) than the wild type and an altered ratio of muramic acid substituents having 37.0, 46.3, and 12.3% δ-lactam, tetrapeptide, and single L-alanine, respectively. This suggests a role for the DacB protein (penicillin-binding protein 5*) in cortex biosynthesis. The sporulation-specific putative peptidoglycan hydrolase CwlD plays a pivotal role in the establishment of the mature spore cortex structure since strain AA107 (*cwlD*) has spore peptidoglycan which is completely devoid of muramic acid δ-lactam residues. Despite this drastic change in peptidoglycan structure, the spores are still stable but are unable to germinate. The role of δ-lactam and other spore peptidoglycan structural features in the maintenance of dormancy, heat resistance, and germination is discussed.

Dormant bacterial endospores formed by the genera *Bacillus* and *Clostridium* are the most resistant living structures known and are able to survive thousands if not millions of years (9). During the quiescent state, spores exhibit high-level resistance to many treatments, including heat, UV light, desiccation, and the action of deleterious chemicals. As a result of their resistance properties, spores are able to survive many food preservation and pasteurization procedures and thus cause huge problems to the food industry (11).

Endospores are characterized by a relatively dehydrated protoplast encased in integument layers (20). The most prominent of the integuments are the spore coat layers which determine the physical properties of the spore surface and are responsible for resistance to enzymatic assault (56). However, the spore coats are not involved in the maintenance of dormancy and heat resistance (56). Between the spore coats and the protoplast membrane is a thick layer of bacterial peptidoglycan, consisting of two sublayers. Innermost is the thin primordial cell wall, so called because it has been proposed that after germination, it probably forms the template for the peptidoglycan of the outgrowing new vegetative cell wall (10, 50). The primordial cell wall peptidoglycan retains the same basic structure as that of the vegetative cell wall (56). The much thicker outer layer of peptidoglycan in the spore is known as the cortex. In most endospores, cortical peptidoglycan is made from the same amino acids and sugar constituents that are found in vegetative cell wall peptidoglycan, but it has several unique spore-specific features. The most prominent of these is the substitution of about 50% of the disaccharides with muramic acid δ-lactam residues (57, 58). The δ-lactam is not randomly located in the glycan chain but occurs predominantly at every alternate disaccharide (49). The remainder of the muramic acid residues are either substituted with a tetrapeptide of L-alanine–D-glutamic acid–*meso*-diaminopimelic acid–D-alanine (30 to 35%) or a single L-alanine substituent with a free carboxyl group (15 to 20%) (49, 57, 58). Spore cortex peptidoglycan of *Bacillus subtilis* has a low degree of cross-linking at only 6 to 9% per disaccharide, which contrasts with 33% in vegetative cell wall peptidoglycan (17, 49). There is some controversy, however, as to whether the low cortical cross-linkage value is due to the method of sample preparation (34, 38). The uncross-linked peptide side chains in the spore cortex of *B. subtilis* are tetrapeptides ending in a single D-alanine, whereas the uncross-linked vegetative cell wall peptide side chains are tripeptides (49).

It has been proposed that the spore cortex is involved in the maintenance but not the establishment of the heat-resistant, dormant state (15). This is likely to be mediated by the ability of the cortex to prevent rehydration of the spore core (21). Greater than 90% of wild-type cortex levels of *Bacillus sphaericus* are necessary for spore heat resistance (25, 26). About 25 and 90% of wild-type cortex levels were found to be necessary for octanol and heat resistance, respectively (25). Further evidence for the role of the cortex in heat resistance comes from the study of the sporulation-specific penicillin-binding protein PBP 5* (47, 52). A *dacB* (encoding PBP 5*) strain produces spores with reduced heat resistance (6, 37). Also, the appearance of PBP 5* during sporulation of a strain bearing

* Corresponding author. Mailing address: Department of Molecular Biology and Biotechnology, University of Sheffield, Firth Court, Western Bank, Sheffield S10 2TN, United Kingdom. Phone: 44 114 282 4411. Fax: 44 114 272 8697. Electronic mail address: s.foster@sheffield.ac.uk.

TABLE 1. *B. subtilis* 168 strains

Strain	Genotype[a]	Origin (reference)
HR	*trpC2*	Laboratory stock
AA101	*trpC2* Δ*pbpE*::Ery^r	PS1805 (39)→HR[b]
AA102	*trpC2 pbpF*::Cm^r	PS1838 (40)→HR
AA103	*trpC2* Δ*pbpD*::Ery^r	PS2022 (41)→HR
AA104	*trpC2 spmB*::Cm^r	PS2029 (37)→HR
AA105	*trpC2 spmA*::Cm^r	PS2030 (37)→HR
AA106	*trpC2 ponA*::Cm^r	PS2031 (42)→HR
AA107	*trpC2 cwlD*::Cm^r	ADD1 (44)→HR
AA108	*trpC2 spoVD*::Kan^r	785 (12)→HR
AA109	*trpC2 dacA*::Cm^r	JT175 (53)→HR
AA110	*trpC2 dacB*::Cm^r	CB36 (6)→HR
AA111	*trpC2 pbpB*::Cm^r	SG38::pL92 (61)→HR
AA112	*trpC2 dacF*::Cm^r	MB24::pPP209 (60)→HR
AA113	*trpC2 dacF*::Cm^r	MB24::pPP214 (60)→HR

[a] Abbreviations: Cm, chloramphenicol; Ery, erythromycin-lincomycin; Kan, kanamycin; r, resistant.

[b] Arrow indicates construction by transformation with chromosomal DNA into HR.

the *gerJ* mutation is delayed, which results in spores which are abnormally heat sensitive (55). The exact structural abnormalities of the spore cortex of the *dacB* mutant have not been determined, although this mutant is twice as cross-linked as the wild type (37).

Despite the obvious importance of the spore cortex in such industrially and medically relevant organisms, very little is known about the fine structure of the cortical peptidoglycan and those features which play crucial roles in the maintenance of dormancy and heat resistance. The recent application of high-performance liquid chromatography (HPLC) and mass spectrometry (MS) techniques (2, 13, 22, 35) to the analysis of cell wall peptidoglycan has revealed a high level of peptidoglycan complexity in several species. Subtle changes in peptidoglycan structure in response to antibiotics or as a result of mutations in peptidoglycan biosynthetic enzymes can be resolved by these techniques (13, 30).

In this paper, we report HPLC and MS analyses of the fine structure of *B. subtilis* endospore peptidoglycan. By the study of specific mutants altered in peptidoglycan metabolism, the role of specific cortical features during differentiation has begun to be elucidated.

MATERIALS AND METHODS

Bacterial strains, growth, and purification of spores. The strains of *B. subtilis* used are shown in Table 1. Vegetative cells of *B. subtilis* 168 were grown in nutrient broth or on nutrient agar plates. Sporulation was initiated in CCY medium, and spores were purified (>99% phase-bright free endospores) as described previously (48). All *B. subtilis* strains used for peptidoglycan analysis were isogenic in the HR background and were made by transformation with the appropriate donor chromosomal DNA (5). When appropriate, chromosomal drug resistance markers in *B. subtilis* were selected with chloramphenicol (5 μg ml^{-1}), kanamycin (10 μg ml^{-1}), or erythromycin (1 μg ml^{-1}) and lincomycin (25 μg ml^{-1}).

Preparation of cortex by chemical extraction of dormant spores. Purified spores (800 mg [dry weight]) were incubated at 100°C for 16 min and then at 37°C for 40 min in 12 ml of extraction buffer (50 mM Tris-HCl [pH 8.0], 4% [wt/vol] sodium dodecyl sulfate [SDS], 30 mM dithiothreitol, 2 mM EDTA). Extracted spores were then washed with warm (37°C) distilled water by centrifugation (14,000 × *g*, 8 min, room temperature) and resuspension, until free of SDS (five washes). Spores were then incubated in 6 ml of a mixture containing 50 mM Tris-HCl (pH 7.0) and 2 mg of pronase ml^{-1} (self-digested at 37°C for 1 h) at 60°C for 90 min prior to centrifugation and resuspension as described above. Spores were then incubated in extraction buffer (at pH 7.0) at 100°C for 16 min and washed as described above. Peptidoglycan-containing insoluble material was finally resuspended in MilliQ water and stored at −20°C.

Preparation of cortex by physical disruption of spores and chemical extraction of integuments. Dormant spores (600 mg at 15 mg ml^{-1}) were refluxed at 85°C for 15 min in 85% (vol/vol) propan-2-ol to inactivate autolytic enzymes (28). Spores were washed by centrifugation (14,000 × *g*, 8 min, room temperature) and resuspension in distilled water followed by breakage in a Braun homogenizer (total of 3 min of homogenization) as described previously (28). Insoluble integuments were extracted by incubation at 100°C in 12 ml of 50 mM Tris-HCl (pH 7)–4% (wt/vol) SDS–30 mM dithiothreitol–2 mM EDTA for 16 min. Integuments were then washed extensively as described above prior to storage in MilliQ water as described above.

Enzymatic hydrolysis of cortex. Samples were digested at 37°C with 250 μg of Cellosyl (gift from R. Marquardt, Hoechst AG, Frankfurt, Germany) ml^{-1} in 25 mM sodium phosphate buffer (pH 5.6) for 15 h. The reaction was stopped by boiling the sample for 3 min. Insoluble material was removed by centrifugation (14,000 × *g*, 8 min, room temperature), and the resulting cortex hydrolysate was stored at −20°C.

HPLC separation of cortical muropeptides. All subsequent treatments were carried out with MilliQ water. Muropeptide-containing samples were reduced as described previously (14), by using sodium borohydride at 1.66 mg ml^{-1} (final concentration), and the reaction was carried out for exactly 8 min. The reduced muropeptides were then separated by reverse-phase HPLC (RP-HPLC). A Hypersil octadecylsilane column from Sigma, Poole, United Kingdom (4.6 by 250 mm; particle size, 5 μm) was used without a guard column. All samples were filtered (0.45-μm pore size) prior to analysis to remove insoluble material. Elution buffers were as follows: A, 40 mM sodium phosphate (pH 4.23 at 20°C); B, 40 mM sodium phosphate (pH 4.1 at 20°C)–20% (vol/vol) methanol. The column was equilibrated in buffer A (0.59 ml min^{-1}) at 40°C with a Waters 600E delivery system and column heater. The muropeptide-containing samples (50 μl) were then loaded by injection (Waters 717 plus autosampler). A linear gradient of from 0 to 100% buffer B over a period of 160 min was started at the moment of injection; this was followed by isocratic elution with 100% buffer B for a further 40 min. The flow rate was linearly decreased from 0.59 to 0.50 ml min^{-1} over the course of the gradient. The eluted compounds were detected by monitoring A_{202} (Waters 486 absorbance detector), and muropeptides were collected individually at the detector outlet.

Desalting of HPLC-separated muropeptides. Individual muropeptide-containing fractions were freeze-dried and resuspended in water. Muropeptides were desalted by HPLC chromatography with Hypersil octadecylsilane column identical to that used for the initial separation. The column was equilibrated with 0.007% (vol/vol) trifluoroacetic acid (Sigma) at 35°C with a flow rate of 1 ml min^{-1} prior to injection of the sample (1.8 ml). Muropeptides were eluted with a linear gradient (0 to 100%) initiated at the time of injection of 50% (vol/vol) methanol–0.0025% (vol/vol) trifluoroacetic acid over 30 to 50 min (depending on the hydrophobicity of the muropeptide). Muropeptides were detected at 202 nm.

Amino acid analysis. The Pico-Tag amino acid analysis system (Waters) was used. Prior to amino acid analysis, desalted, HPLC-purified muropeptides were hydrolyzed with 4 M HCl for 14 h at 100°C. All other samples were hydrolyzed with 5 M HCl for 14 h at 110°C. The hydrolysates were dried and derivatized with phenylisothiocyanate as recommended at 110°C. The phenylthiocarbamyl amino acid derivatives were separated on an HPLC Pico-Tag column (Waters; 3.9 by 150 mm) maintained at 38°C. Peaks were detected at 254 nm and integrated by use of a Waters 746 data module integrator.

Californium-252 plasma desorption linear time-of-flight MS. Positive and negative ion plasma desorption mass spectra were obtained as described previously (2, 43).

Matrix-assisted laser desorption-ionization reflectron time-of-flight MS. MS measurements were performed in the reflection mode on a Katros Analytical Kompact MALDI III (Katros Analytical, Manchester, United Kingdom) laser desorption time-of-flight instrument equipped with a nitrogen UV laser (λ = 337 nm; 3-ns pulse width). Positive- and negative-ion mass spectra were obtained by signal averaging of 50 consecutive laser shots. During data acquisition, the shot-to-shot signal was viewed on the computer monitor since the laser was attenuated to maintain the optimal laser power density near the threshold level. The final ion acceleration potential was ±20 kV. Conversion of flight time to mass/charge ratio was achieved by external calibration with the $[M + H]^+$ or $[M - H]^-$ peak of gentisic acid (Sigma), α-cyano-4-hydroxy cinnamic acid (Sigma), Leu-Trp-Met-Arg-Phe-Ala (Serva, Heidelberg, Germany), oxytocin, LHRH, bee venom mellitin, somatostatin, and bovine insulin (Sigma). Sample preparation was performed for all samples (apart from muropeptide 17) in a manner similar to the reported procedure (3, 4). A saturated solution of the matrix gentisic acid was prepared in acetonitrile-water (70:30 [vol/vol]), and 100 μl of this solution was diluted by adding 300 μl of acetonitrile-water (70:30 [vol/vol]) to be used as the final matrix solution. For MS analysis of muropeptide 17, the thin-layer sample preparation technique with α-cyano-4-hydroxy cinnamic acid as the matrix was applied (54).

HPLC-desalted muropeptides were dissolved in 7 μl of 0.1% trifluoroacetic acid. Five microliters of each sample was mixed on the disposable sample probe with 0.5 μl of matrix solution and allowed to dry in the system apparatus before insertion into the MS.

FDNB determination of peptidoglycan cross-linking. Spore samples were chemically extracted as described above with an additional step (incubation for 6 min at 90°C in 5% [vol/vol] trichloroacetic acid) performed before pronase hydrolysis. The samples (100 μl; 3 mg ml^{-1}) were treated with 1-fluoro-2,4-dinitrobenzene (FDNB) as described previously (33). Incubation in the presence

of FDNB was carried out overnight by continuous shaking of samples at room temperature. FDNB-treated samples and controls were washed three times by centrifugation (14,000 × *g*, 8 min, room temperature) and resuspension prior to amino acid analysis as described above.

The cross-linking index was determined by calculation of the ratio of cross-linked to total diaminopimelic acid (Dpm) amino termini. This was done by amino acid analysis as described above (dinitrophenyl Dpm being unable to be labelled by phenylisothiocyanate). The amount of Dpm was expressed in a ratio to that of a well-resolved amino acid (valine) (38).

RESULTS

Optimization of conditions for *B. subtilis* spore muropeptide production. Several chemical extraction procedures have been used to solubilize the *B. subtilis* spore coat (36, 62). However, preliminary tests indicated that high temperature combined with extraction of spore coat proteins at >pH 8 caused structural alterations to the glycan strands of the peptidoglycan, leading to deacetylation of muropeptides and opening of the δ-lactam ring.

Cellosyl is a muramidase produced by *Streptomyces coelicolor* which is able to efficiently hydrolyze bacterial peptidoglycan (19). Electron microscopy of Cellosyl-hydrolyzed, permeabilized spores revealed that the cortex and primordial cell wall layers had disappeared but that vestigial coat layers and insoluble core material remained (data not shown).

To investigate the degree of solubilization of the peptidoglycan, the relative levels of the Dpm component (likely to be exclusive to peptidoglycan) were measured in total permeabilized spores and Cellosyl-hydrolyzed soluble and Cellosyl-hydrolyzed insoluble fractions. At least 97% of total permeabilized spore Dpm was solubilized by Cellosyl treatment with <3% contamination with nonpeptidoglycan amino acids. Mutanolysin from *Streptomyces globisporus* (Sigma) and recombinant lysozyme (Sigma) were also found to solubilize the cortex to an extent similar to that of Cellosyl. However, the soluble fraction from the digests was contaminated to a higher degree with nonpeptidoglycan amino acids.

Effect of reduction conditions on spore muropeptides. Spore cortex structural analysis by Warth and Strominger (57, 58) showed that, in addition to reduction at the C-1 of muramic acid, sodium borohydride readily reduced the lactyl side chain in the muramic δ-lactam residue, yielding at least two products with differing properties. In this study, reduction was initially carried out with 5 mg of sodium borohydride ml^{-1} (final concentration) over a 15-min reaction time. Under these conditions, a large number of muropeptides were resolved by HPLC. The amino acid and MS analyses later revealed that some of the muropeptides had been generated by the reduction of the lactyl side chain (57, 58). Indeed, for predominant muropeptides with a high δ-lactam content (i.e., hexasaccharide), at least three different products from each muropeptide were identified. This problem was greatly alleviated by use of a shorter reduction time (8 min) and by lowering the final concentration of sodium borohydride to 1.66 mg ml^{-1}. This modification of the method did not affect the reduction of the C-1 of muramic acid.

HPLC analysis of Cellosyl-solubilized spore muropeptides. Soluble spore muropeptides produced by Cellosyl digestion were separated by RP-HPLC, and a representative chromatogram is shown in Fig. 1A. The chromatography conditions led to the resolution of more than 20 distinct muropeptides. The relatively small number of peaks indicated a somewhat simple peptidoglycan structure. The size of peaks 4 and 5 (Fig. 1A) was greatly affected by the method of spore permeabilization, being very much more prominent if extracted at a high pH (>9) and a high temperature for long periods (>20 min) or if a trichloroacetic acid extraction step was included. These muropeptides are unlikely to occur naturally in spores and are probably generated as artifacts by the treatment process. Twenty-four well-resolved muropeptides indicated in Fig. 1A were collected from a series of identical separations for analysis and identification. The muropeptide profile remained essentially constant both in peak retention time and relative peak heights for at least five independent spore preparations and extractions. Additional muropeptides were not resolved over longer elution times or by the use of 25% (vol/vol) methanol in buffer B.

Omission of the pronase digestion step during spore permeabilization or addition of pronase digestion just prior to peptidoglycan hydrolysis did not affect the muropeptide profile, and so there does not seem to be significant levels of protein strongly associated with, or covalently bound to, the peptidoglycan. Also, hydrofluoric acid treatment (48% [vol/vol], 4°C, 24 h) of permeabilized spores had no effect on the profile. Hydrofluoric acid is known to hydrolyze the linkage between secondary anionic polymers (teichoic and teichuronic acid) and peptidoglycan (27). This confirms the lack of such polymers covalently bound to the spore cortex peptidoglycan (28, 58).

Effect of mechanical spore disruption on muropeptide profile. It has been speculated that mechanical disruption of spores, by breakage with glass beads, may cause structural alterations to the spore peptidoglycan, thus complicating interpretation (34). The muropeptide profiles of peptidoglycan prepared by chemical extraction and by mechanical disruption (plus chemical extraction) were compared (data not shown). Both profiles were comparable in peak numbers and amounts. Evidently, the shear forces during mechanical breakage do not significantly disrupt the peptide bonds of the cortical peptidoglycan.

Structural identification of the spore muropeptides. Samples containing muropeptides in the numbered peaks in Fig. 1A were collected and desalted by HPLC as described in Materials and Methods. Each muropeptide was then identified by a combination of amino acid and MS analyses.

Amino acid analysis of the 24 muropeptides revealed them all to be peptidoglycan derived (Table 2). The only amino acids detected were Ala, Glu, and Dpm, which are the expected constituents of spore cortex peptidoglycan (58). Glu and Dpm were always present in equimolar amounts, while Ala was variable between muropeptides, in some being the only amino acid present (e.g., muropeptides 2 and 11). The amino sugars glucosamine and muramic acid were found in all samples; however, the method used for amino acid analysis was not appropriate for their quantification. The relative amounts of amino sugars in each muropeptide given in Table 2 have been calculated after MS analysis.

The determination of the precise relative molecular masses of the various muropeptides was crucial for determination of their structures. The HPLC-desalted peptidoglycan fragments were analyzed by positive- and negative-ion plasma desorption MS (muropeptides 1 to 21) and matrix-assisted laser desorption-ionization MS (muropeptides 22 to 24). The sodiated molecular ions of the major peptidoglycan monomers and dimers could be detected as dominating ions in the positive-ion mode (Table 2). Additional complex sodium and/or potassium adduct ions, $[M + K]^+$, $[M + 2Na - H]^+$, $[M + 3Na - 2H]^+$, $[M + 4Na - 3H]^+$, and $[M + 5Na - 4H]^+$, were also observed. The negative-ion mass spectra exhibited mostly abundant ions of the type $[M - H]^-$. The sensitivity in the negative-ion mode was significantly higher than that in the positive-ion mode. Low-intensity ions of the type $[M + Na - 2H]^-$ and $[M + 2Na - 3H]^-$ were determined as well. The experimental

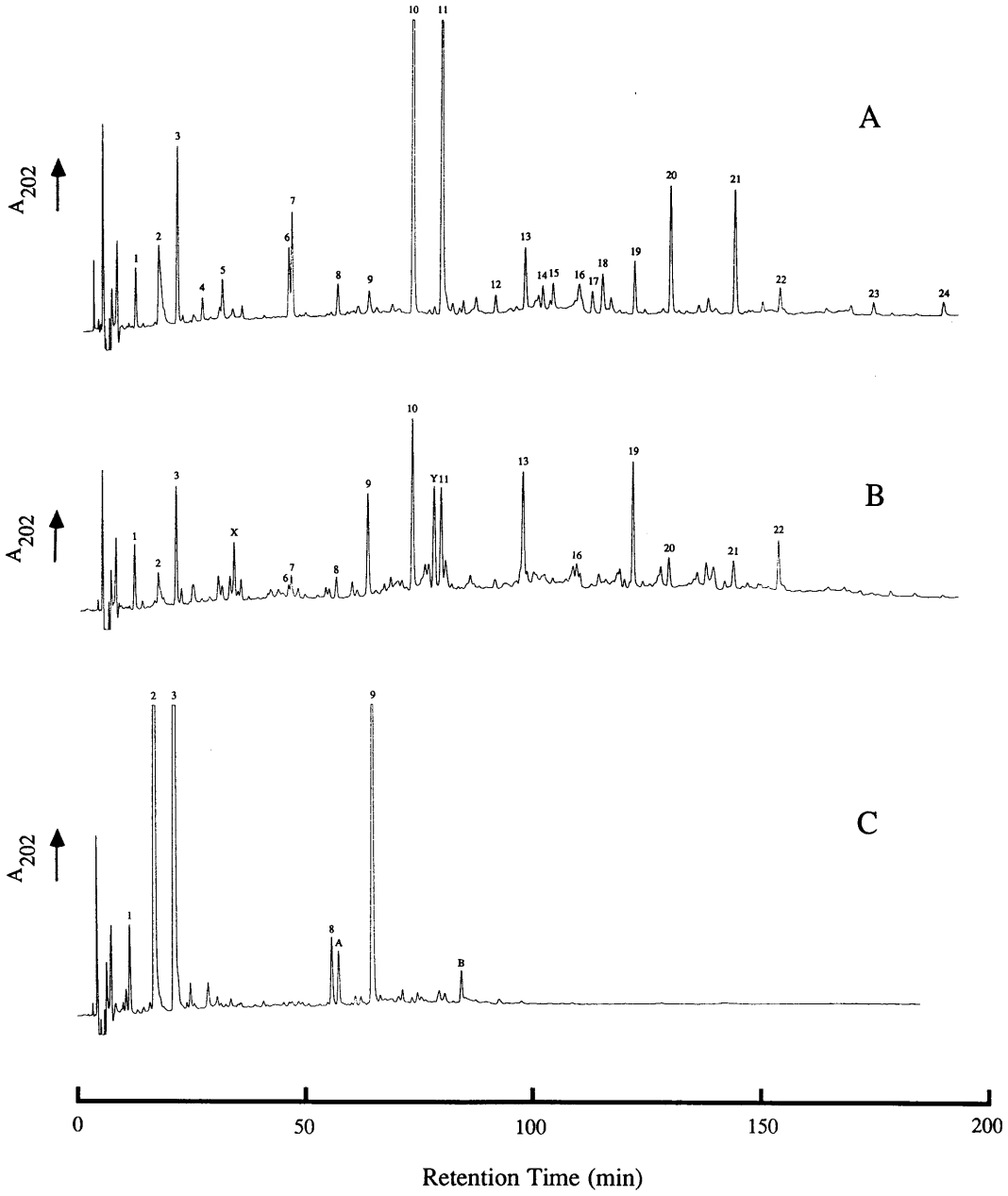

FIG. 1. Analysis of endospore *B. subtilis* peptidoglycan composition by RP-HPLC. Samples of peptidoglycan from endospores of strains HR (wild type) (A), AA110 (*dacB*) (B), and AA107 (*cwlD*) (C) were subjected to HPLC analysis, and the A_{202} of the eluates was monitored. The numbered and lettered peaks correspond to those which were subjected to further analyses.

m/*z* values are compared in Table 2 with values calculated for muropeptides by use of the amino acid composition of the peptidoglycan of *B. subtilis.*

Spore peptidoglycan composition of *B. subtilis*. Amino acid and MS analyses allowed structural determination and quantification of all 24 purified spore muropeptides (Table 3; Fig. 2). Muropeptides were quantified (Table 3) after structural determination by the comparison of relative amounts of alanine in the 24 muropeptides from three different preparations. From the chemical structure assigned to most of the muropeptides (Table 3; Fig. 2), it is evident that the glycosidic bond adjacent to a muramic δ-lactam residue is resistant to Cellosyl. Such refractility to hydrolysis by the action of muramidases has been previously noted (58). Muropeptides 4 to 7, 12, and 14 to 18 are likely to have been produced during permeabilization and reduction, although the procedure was developed to minimize their presence as described above. Opening of the muramic acid δ-lactam ring (muropeptides 4 and 5) results in an approximate increase in molecular mass corresponding to one molecule of water. Reduction of the muramic acid δ-lactam ring (muropeptides 6, 7, 12, and 14 to 17) leads to the loss of an oxygen atom with the gain of two hydrogens.

The dominant cortical muropeptides (Table 3; Fig. 2) are tetrasaccharide alanine (31.0%; addition of muropeptides 4, 6, and 11) and tetrasaccharide tetrapeptide (24.0%; muropeptides 5, 7, and 10). The high relative levels of uncross-linked

TABLE 2. Calculated and observed *m/z* values for sodiated or protonated and deprotonated molecular ions of spore muropeptides

Muropeptide[a]	Ion	*m/z*		Δm (Da)[b]	Error (%)[c]	Muropeptide composition[d]					
		Observed	Calculated			*N*-Glc[e]	*N*-Mur[e]	δ-Mur[e]	Glu	Ala	Dpm
1	$[M + Na]^+$	894.6	893.9	0.7	0.08	1	1	0	1	1	1
	$[M - H]^-$	870.4	869.9	0.5	0.06						
2	$[M + Na]^+$	592.8	592.6	0.2	0.03	1	1	0	0	1	0
	$[M - H]^-$	568.6	568.6	0.0	0.00						
3	$[M + H]^+$	943.5	942.9	0.6	0.06	1	1	0	1	2	1
	$[M - H]^-$	941.1	940.9	0.2	0.02						
4	$[M + Na]^+$	1029.8	1011.0	**18.8**[f]		2	1	1	0	1	0
	$[M - H]^-$	1005.6	987.0	**18.6**							
5	$[M + Na]^+$	1402.5	1383.3	**19.2**		2	1	1	1	2	1
	$[M - H]^-$	1378.3	1359.3	**19.0**							
6	$[M + Na]^+$	997.4	1011.0	**−13.6**		2	1	1	0	1	0
	$[M - H]^-$	973.5	987.0	**−13.5**							
7	$[M + Na]^+$	1369.7	1383.3	**−13.6**		2	1	1	1	2	1
	$[M - H]^-$	1346.0	1359.3	**−13.3**							
8	$[M + Na]^+$	1817.7	1817.8	−0.1		2	2	0	2	3	2
	$[M - H]^-$	1793.5	1793.8	−0.3	−0.02						
9	$[M + Na]^+$	1888.7	1888.9	−0.2	−0.01	2	2	0	2	4	2
	$[M - H]^-$	1864.6	1864.9	−0.3	−0.02						
10	$[M + Na]^+$	1384.0	1383.3	0.7	0.05	2	1	1	1	2	1
	$[M - H]^-$	1361.2	1359.3	1.9	0.14						
11	$[M + Na]^+$	1011.8	1011.0	0.8	0.08	2	1	1	0	1	0
	$[M - H]^-$	987.6	987.0	0.6	0.06						
12	$[M + Na]^+$	1788.1	1801.7	**−13.6**		3	1	2	1	2	1
	$[M - H]^-$	1764.2	1777.7	**−13.5**							
13	$[M + Na]^+$	2308.2	2307.2	1.0	0.04	3	2	1	2	4	2
	$[M - H]^-$	2282.9	2283.2	−0.3	−0.01						
14	$[M + Na]^+$	1415.8	1429.4	**−13.6**		3	1	2	0	1	0
	$[M - H]^-$	1391.4	1405.5	**−14.1**							
15	$[M + Na]^+$	1416.6	1429.4	**−12.8**		3	1	2	0	1	0
	$[M - H]^-$	1392.7	1405.5	**−12.8**							
16	$[M + Na]^+$	2711.8	2725.6	**−13.8**		4	2	2	2	4	2
	$[M - H]^-$	2687.7	2701.6	**−13.9**							
17	$[M + Na]^+$	1787.7	1801.7	**−14.0**		3	1	2	1	2	1
	$[M - H]^-$	1763.5	1777.7	**−14.2**							
18	$[M + Na]^+$	1560.0	1429.4	**130.6**		3	1	2	0	1	0
	$[M - H]^-$	1535.4	1405.4	**130.0**							
19	$[M + Na]^+$	2724.4	2725.6	−1.2	−0.04	4	2	2	2	4	2
	$[M - H]^-$	2699.9	2701.6	−1.7	−0.06						
20	$[M + Na]^+$	1802.3	1801.7	0.6	0.03	3	1	2	1	2	1
	$[M - H]^-$	1778.2	1777.7	0.5	0.03						
21	$[M + Na]^+$	1430.9	1429.4	1.5	0.10	3	1	2	0	1	0
	$[M - H]^-$	1406.1	1405.4	0.7	0.05						
22	$[M + Na]^+$	3141.8	3142.0	−0.2	−0.01	5	2	3	2	4	2
	$[M - H]^-$	3118.4	3118.0	0.4	0.01						
23	$[M + Na]^+$	2218.6	2220.1	−1.5	−0.07	4	1	3	1	2	1
	$[M - H]^-$	2194.6	2196.1	−1.5	−0.07						
24	$[M + Na]^+$	1847.5	1847.8	−0.3	−0.02	4	1	3	0	1	0
	$[M - H]^-$	1823.6	1823.8	−0.2	−0.01						
X	$[M + Na]^+$	1407.5	1408.4	−0.9	−0.06	1	1	0	2	4	2
	$[M - H]^-$	1383.5	1384.4	−0.9	−0.06						
Y	$[M + Na]^+$	1827.4	1826.8	0.6	0.03	2	1	1	2	4	2
	$[M - H]^-$	1803.5	1802.8	0.7	0.04						
A	$[M + Na]^+$	1815.5	1815.8	−0.3	−0.02	2	2	0	2	3	2
	$[M - H]^-$	1792.2	1791.8	0.4	0.02						
B	$[M + Na]^+$	2786.7	2788.8	−2.1	−0.07	3	3	0	3	6	3
	$[M - H]^-$	2810.9	2812.8	−1.9	−0.07						

[a] Muropeptides are numbered as indicated in Fig. 1.
[b] Difference between observed and calculated sodiated or deprotonated molecular mass values.
[c] Calculated as [(observed mass − calculated mass)/calculated mass] × 100.
[d] Ratios of amino acids are derived from the experimental data rounded to the nearest whole number. Amino sugar values were calculated after MS analysis.
[e] Abbreviations: *N*-Glc, *N*-acetylglucosamine; *N*-Mur, *N*-acetyl muramic acid; δ-Mur, muramic acid δ-lactam.
[f] Boldface characters denote *m/z* values calculated as the most likely combinations of the list components which nevertheless deviated largely from the observed values.

tetrasaccharides compared with that of disaccharides, hexasaccharides, or octasaccharides (Table 3) indicated that the δ-lactam moiety was not randomly located in the glycan chain but occurred predominantly on alternate disaccharides as has been proposed previously (58).

Disaccharide tripeptide (muropeptide 1) and disaccharide tripeptide disaccharide tetrapeptide (muropeptide 8) represent 4.2% of the total muropeptides (Table 3). These two muropeptides, which lack muramic acid δ-lactam residues, have tripeptide side chains which may be more indicative of

TABLE 3. Muropeptide identities and composition of spore peptidoglycan from *B. subtilis* HR, AA110 (*dacB*), and AA107 (*cwlD*)

Muropeptide[a]	Retention time (min)	Identity[b]	Mol%[c]		
			HR (wild type)	AA110 (*dacB*)	AA107 (*cwlD*)
1	11.6	Disaccharide tripeptide	3.1	7.8	1.8
2	17.2	Disaccharide alanine	5.9	5.0	40.7
3	21.2	Disaccharide tetrapeptide	10.3	15.4	50.8
4	26.8	Tetrasaccharide alanine with open lactam	1.8		
5	31.2	Tetrasaccharide tetrapeptide with open lactam	1.8		
6	46.4	Tetrasaccharide alanine with reduced lactam	5.4	2.7	
7	47.2	Tetrasaccharide tetrapeptide with reduced lactam	4.4	2.1	
8	57.2	Disaccharide tripeptide disaccharide tetrapeptide	1.1	1.4	0.8
9	64.4	Disaccharide tetrapeptide disaccharide tetrapeptide	0.6	6.0	5.1
10	74.4	Tetrasaccharide tetrapeptide	17.8	13.1	
11	81.2	Tetrasaccharide alanine	23.8	14.6	
12	92.2	Hexasaccharide tetrapeptide with one reduced lactam	1.1		
13	99.2	Disaccharide tetrapeptide tetrasaccharide tetrapeptide	2.6	8.5	
14	100.8	Hexasaccharide alanine with one reduced lactam	1.1		
15	105.5	Hexasaccharide alanine with one reduced lactam	1.1		
16	111.2	Tetrasaccharide tetrapeptide tetrasaccharide tetrapeptide with one reduced lactam	0.3	0.6	
17	114.0	Hexasaccharide tetrapeptide with one reduced lactam	1.1		
18	116.2	Hexasaccharide alanine with three acetylations and one reduced lactam[d]	2.2		
19	123.6	Tetrasaccharide tetrapeptide tetrasaccharide tetrapeptide	0.8	4.7	
20	131.6	Hexasaccharide tetrapeptide	5.8	3.3	
21	146.0	Hexasaccharide alanine	6.0	3.5	
22	156.0	Tetrasaccharide tetrapeptide hexasaccharide tetrapeptide	0.5	2.0	
23	176.8	Octasaccharide tetrapeptide	0.6		
24	192.4	Octasaccharide alanine	0.8		
X	34.0	Disaccharide tetrapeptide tetrapeptide		2.5	
Y	79.2	Tetrasaccharide tetrapeptide tetrapeptide		6.8	
A	59.2	Disaccharide tripeptide disaccharide tetrapeptide with amidation			0.6
B	86.0	Disaccharide tetrapeptide disaccharide tetrapeptide disaccharide tetrapeptide			0.2

[a] Muropeptides are numbered as indicated in Fig. 1.
[b] Selected structures are diagrammatically represented in Fig. 2.
[c] Moles percent calculated after amino acid analysis and integrated area values for muropeptides from the total Cellosyl digest and pure muropeptides.
[d] Probable minor reduction form, all others being in the major form (57).

vegetative cell wall than of spore cortex (49). Thus, these are possibly derived from the primordial cell wall, which constitutes a small proportion of the total spore peptidoglycan (10).

Muropeptide 18 has amino acid and sugar compositions identical to those of muropeptide, 21 although it has a different retention time (Fig. 1A; Tables 2 and 3). MS revealed an anomalous increase in mass of 130 Da, which may be due to three acetylation events and one muramic acid δ-lactam residue reduction to the minor form (57).

Muropeptides 14 and 15 have identical amino acid contents and molecular masses but show different retention times, 100.8 and 105.5 min, respectively (Fig. 1A; Table 3). They are both hexasaccharide alanine with one reduced muramic acid δ-lactam. The anomaly in retention time may be due to the reduction occurring on different muramic acid δ-lactam residues in each muropeptide. Equivalent alternative reduction sites would also explain the retention times of the otherwise seemingly identical muropeptides 12 and 17.

Interpretation of all of the muropeptide data (Table 3) reveals key features of the overall peptidoglycan structure (Table 4). Of the muramic acid residues, 25.7 and 23.3% are substituted with a tetrapeptide or a single alanine residue, respectively. Muramic acid δ-lactam residues account for 49.0% of total substituents. The cross-linking index is only 11.4% per Dpm residue (as calculated from the muropeptide analysis) and because of the low levels of tetrapeptides is actually only 2.9% per muramic acid residue. The cross-linking index was determined independently by estimation of the amounts of Dpm present in acid hydrolysates, with or without the reaction of the free amino groups with FDNB, prior to quantitation by phenylisothiocyanate derivatization. An index of 20% per Dpm residue was found (Table 4).

Analysis of the role of peptidoglycan biosynthetic enzymes and autolysins in the determination of spore peptidoglycan structure. To elucidate the role of peptidoglycan biosynthetic and modification enzymes in the creation of the spore peptidoglycan, the muropeptide profile was examined for a number of strains bearing mutations in genes encoding components either known or proposed to have a role in peptidoglycan biosynthesis or maturation. All of the mutations were transferred to the isogenic background of strain HR to prevent any extraneous strain differences.

The *dacB* gene encodes the sporulation-specific PBP 5*, and the spore muropeptide profile of strain AA110 (*dacB*) is shown in Fig. 1B. Upon comparison of strains AA110 and HR (wild type), a number of muropeptide changes both in composition and relative amounts are found. Muropeptides 9, 13, 19, and 22 increased in amount in AA110, and most others decreased (Fig. 1B). Also, two novel muropeptide species are present in amounts which have allowed identification (Fig. 1B) (muropeptides X and Y). These have been identified as disaccharide tetrapeptide tetrapeptide (X) and tetrasaccharide tetrapeptide tetrapeptide (Y) (Tables 2 and 3; Fig. 2).

Quantification of the spore muropeptides from AA110 (Tables 3 and 4) reveals that the peptidoglycan has cross-linking indexes of 31.2 and 58% (per Dpm residue) as measured by HPLC and FDNB analyses, respectively (Table 4). This level of cross-linking is approximately three times (per Dpm) as much

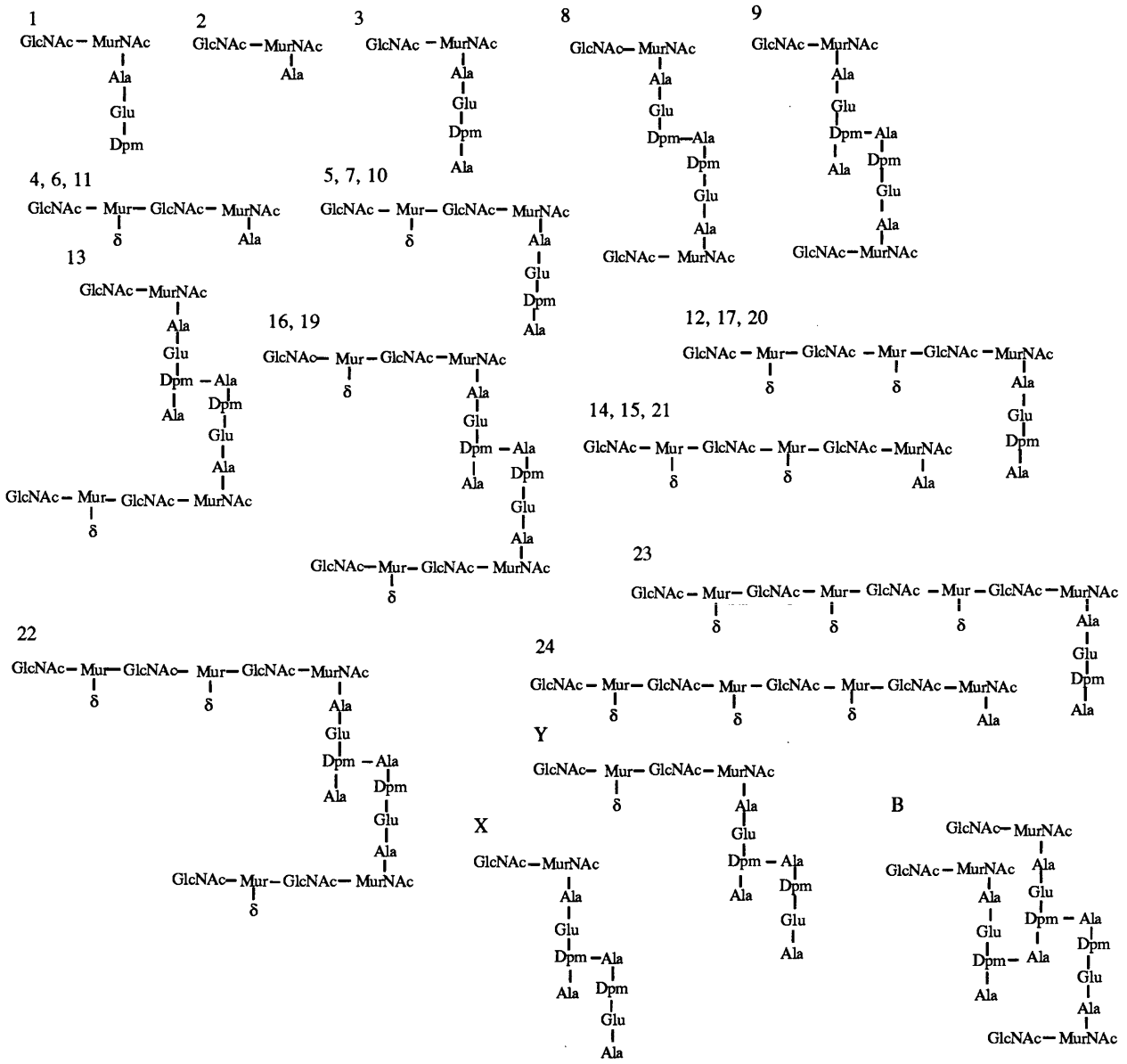

FIG. 2. Structure of *B. subtilis* spore muropeptides. Muropeptides are labelled as in Fig. 1 and Tables 2 and 3. Abbreviations: GlcNac, *N*-acetylglucosamine; MurNac, *N*-acetylmuramic acid; Mur, muramic acid; δ, δ-lactam residue.

as in the parental peptidoglycan and five times greater per muramic acid. Table 4 shows that 46.3% of the muramic carboxyls are substituted with tetrapeptide, 12.3% are substituted with alanine, and approximately 37.0% are lactamized in AA110. Thus, the increase in muropeptide dimers (Table 3) is due not only to a higher proportion of the available tetrapeptides being cross-linked but also to a higher number of the muramic acid residues being substituted with tetrapeptides. This occurs at the expense of both single alanine substituents and δ-lactam residues. The increase in peptidoglycan cross-linking cannot be accounted for by a polar effect of the *dacB* mutation on downstream genes in the operon, since peptidoglycan from AA104 (*spmB*) showed in fact approximately half the cross-linking of that of the parent (data not shown). AA105 (*spmA*) failed to yield stable endospores (three independent preparations for muropeptide analysis).

The *cwlD* gene has been proposed to encode a sporulation-specific peptidoglycan hydrolase which may have a role in cortex maturation or germination (44). The muropeptide profile of strain AA107 (*cwlD*) is shown in Fig. 1C. This single mutation leads to a dramatic alteration in peptidoglycan structure. Overall, there are in fact only a few constituent muropeptides. Muropeptides 2, 3, and 9 have increased enormously in amount compared with the parent, and nearly all others have disappeared entirely (Fig. 1C; Table 3). Two new muropeptides (A and B) were identified and characterized (Fig. 1C and 2; Tables 2 and 3). Muropeptide A is disaccharide tripeptide disaccharide tetrapeptide, with the free carboxyl group of the uncross-linked Dpm probably amidated as is found in vegetative cell wall peptidoglycan of *B. subtilis*. Muropeptide B is a trimer of disaccharide tetrapeptide disaccharide tetrapeptide disaccharide tetrapeptide.

TABLE 4. Cross-linking index and muramic acid substitution of *B. subtilis* spore peptidoglycan

Strain	Cross-linking index (%)[a]				Muramic acid substitution (%)[b]			
	HPLC		FDNB		Tri	Ala	Tetra	δ-Mur
	Mur	Dpm	Mur	Dpm				
HR (wild type)	2.9	11.4	5.0	20.0	2.0	23.3	25.7	49.0
AA110 (*dacB*)	14.4	31.2	26.9	58.0	4.4	12.3	46.3	37.0
AA107 (*cwlD*)	6.5	11.0	11.6	20.2	3.0	38.2	58.8	0

[a] Calculated as described in Materials and Methods from FDNB analysis or HPLC muropeptide quantification (Table 3) and expressed as a percentage per Dpm or per muramic acid residue [(Dpm cross-linking value) × (fraction of total muramic acid residues with Dpm in side chain)].

[b] Abbreviations: Tri, tripeptide; Ala, alanine; Tetra, tetrapeptide; δ-Mur, muramic acid δ-lactam, Mur, muramic acid.

The striking changes in the cortex structure in the *cwlD* mutant are due to the total lack of muramic acid δ-lactam residues in the peptidoglycan (Tables 3 and 4). Disaccharide alanine and disaccharide tetrapeptide represent 91.5% of the total muropeptides (Table 3). The cross-linking index per Dpm residue, estimated by HPLC-eluted muropeptides or by FDNB, was found to be similar to that of the wild type (Table 4), suggesting that the *cwlD* mutation has no effect on peptidoglycan cross-linking. However, when the cross-linking index is calculated per muramic acid residue, the value is approximately double that of the parent strain.

The spore muropeptides from strains AA109 (*dacA*) (53), AA101 (*pbpE*) (39), AA102 (*pbpF*) (40), AA103 (*pbpD*) (41), AA111 (*pbpB*) (61), AA112 (*dacF*) (60), AA113 (*dacF*) (60), and AA106 (*ponA*) (42) were also analyzed. No significant alterations in composition or relative amounts of muropeptides were observed.

DISCUSSION

Core dehydration is pivotal in the ability of bacterial endospores to withstand extremely high temperatures and remain dormant for prolonged periods of time (15). This dehydration is maintained by the spore cortex peptidoglycan (21). The key to the ability of the cortex to fulfill this role is determined by its structure. We have elucidated the fine structure of the cortex peptidoglycan of *B. subtilis* 168 and begun to define the importance of specific structural features during differentiation.

Early work determined the basic chemical constituents of spore cortex and revealed it to be unique among the bacterial peptidoglycans (49, 57, 58). The most prominent feature is the presence of the δ-lactam group on 50% of the muramic acid residues (57, 58). This concurs well with our figure of 49% (Table 4). The δ-lactam group occurs on mostly every alternate muramic acid and renders the adjacent bond resistant to muramidase digestion (Fig. 2; Table 3) (57, 58). Warth and Strominger (57, 58) found 20 and 30%, compared with 23.3 and 25.7% in our study, of the muramic acid residues substituted with a single L-alanine and tetrapeptide, respectively. The low proportion of muramic acid residues bearing tetrapeptide substituents (25.7%) (Table 4) contributes at least in part to the relatively uncross-linked nature of the cortex. We measured the cross-linking index by two independent methods, both of which gave low values, although the FDNB method gave a value roughly twice that obtained by calculation from the muropeptides separated by HPLC (FDNB, 20% per Dpm; HPLC, 11.4% per Dpm) (Table 4). By using FDNB, Warth and Strominger (58) found a 19% cross-linking index, whereas Popham and Setlow (38) reported a value of 37%. This discrepancy may be due to strain differences or the protocol used to produce spore cortex. The lower cross-linking index measured by HPLC may well be more accurate than the FDNB value. The higher cross-linking index measured by FDNB may be due to the fact that in the permeabilized spore, FDNB may not be able to access all of the free Dpm amino groups embedded in the cortex. It is also possible that higher oligomers, whose absence would lead to a lower cross-linking index estimation, are not eluted from the HPLC column by our protocol. However, longer elution times and increases in the organic solvent concentration in the buffer did not reveal any additional muropeptides in significant amounts. It is important to note that particularly for spore peptidoglycan, the method of calculation of the cross-linking index has a dramatic effect on the value obtained. This is due to the fact that in spore peptidoglycan, only 25.7% of the muramic acid residues are substituted with a tetrapeptide side chain (which contains Dpm). Thus, per muramic acid in the glycan chain, the cross-linking value is fourfold less than the value obtained per Dpm residue. The more accurate representation of cross-linking is the per muramic acid value since this does not need to be qualified with further information as to the substituent status of the peptidoglycan. The relevance of this comes when comparing spore peptidoglycan with vegetative cell peptidoglycan, which has essentially 100% of the muramic acid residues substituted with a peptide containing Dpm. The spore peptidoglycan is approximately 11-fold less cross-linked than vegetative cell wall (2.9% [Table 4] versus 33% [17]) when calculated per muramic acid. From this initial structural analysis, it is not clear what role this incredibly low level of cortex cross-linking has during differentiation.

O-Acetylation of peptidoglycan occurs in gram-positive (46) and gram-negative (35) bacteria but has not been reported previously in endospore peptidoglycan. The shift in the molecular weight in the assigned structure of muropeptide 18 (Fig. 1A; Table 2) corresponds to three possible acetyl groups and one muramic acid δ-lactam residue reduction (Table 3). The same product was present in high amounts in *Bacillus megaterium* cortex (data not shown). The presence of other muropeptides in *B. megaterium* with a corresponding shift in molecular mass of multiples of 42 Da supports the possibility of acetylation. Further analysis by incubation of *B. subtilis*-permeabilized spores in 0.1 M NaOH, a treatment known to hydrolyze *O*-acetyl groups, was unsuccessful since the muramic acid δ-lactam residues were destroyed.

The muropeptides containing tripeptide side chains may be part of the primordial cell wall (Table 3), since this has been proposed to retain the structure of the vegetative cell wall peptidoglycan (10). A previous study (10) has suggested that up to 20% of the spore peptidoglycan is primordial cell wall. Our results suggest a much lower value at only 2% (Table 4). It is unlikely that this peptidoglycan layer plays a role in dormancy but instead it is likely that it remains after the cortex is hydrolyzed during germination and forms the basis of the new wall of the outgrowing, vegetative cell (10).

The ability of spore cortex to maintain dormancy is determined by structural features produced during sporulation. The anisotropic swelling theory of cortex expansion during sporulation states that the cortex layer is first synthesized and then subsequent selective enzymatic cleavage of the peptide cross-links results in radial expansion causing inward mechanical pressure on the spore core (1, 56). Selective hydrolysis of the cortex during germination would release the physical constraint and allow uptake of water. The presence of single L-alanine substituents and muramic acid δ-lactam residues sug-

gests that the cortex is modified after biosynthesis to allow it to mature and take on its final conformation. Cortex biosynthesis involves a machinery similar to that of vegetative cell wall peptidoglycan but with the use of several spore-specific components. Several spore-specific penicillin-binding proteins which have been proposed to have a role in cortex biosynthesis have been identified either biochemically or by sequence homology (12, 47, 53). PBP 5* from *B. subtilis* was purified by affinity chromatography and found to have DD-carboxypeptidase activity in vitro (51). This enzyme is located primarily in the outer forespore membrane, and its transcription is under the control of the mother-cell-specific sigma factor, σ^E (7, 8). It is likely that cortex biosynthesis is driven from the mother cell, and so it was proposed that PBP 5* is involved in cortex production (8, 31, 50). The structural gene encoding PBP 5* designated *dacB* has been studied and inactivated (6, 7). The *dacB* gene is the first member of a tricistronic operon, all three gene products having a role in heat resistance (37). Mutations in the other two genes in the operon (*spmA* and *spmB*) have the most marked effect on heat resistance, but their role in differentiation is unknown (37). Initial results suggested that the *dacB* mutation resulted in cortex with a higher degree of cross-linking than that of the parent and with more peptide side chains (37). Despite the reduced heat resistance of the *dacB* spores, however, the relative water content of the spore core was identical to that of the wild type.

Analysis of the cortical peptidoglycan structure of strain AA110 (*dacB*) revealed that the cross-linking index per muramic acid is five times that of the parental strain (Table 4). This occurs as a result of both an increase in the percentage of tetrapeptides which are cross-linked (31.2%) and an alteration in the muramic acid substituent ratios. The results suggest that the D-Ala–D-Ala carboxypeptidase activity of PBP 5* (51) is involved in regulating the degree of cortex peptide cross-linking, which has been suggested previously (37). Cleavage of the terminal D-alanine from the pentapeptide would leave the peptide unable to function as a donor in D-Ala–Dpm cross-link formation. The absence of muropeptide with a pentapeptide side chain in the *dacB* mutant suggests that another enzyme is responsible for the cleavage of the terminal D-Ala from the pentapeptide unit or alternatively is able to compensate for the loss of PBP 5*. Since cortex from AA110 (*dacB*) still has a high level of δ-lactam residues, it is unlikely that it plays a role, even indirectly, in their production, especially since the increase in tetrapeptide substituents occurs with a concomitant loss of both δ-lactam and single L-Ala residues. AA104 (*spmB*) spore peptidoglycan had half the cross-linking of the parent. Spores of this mutant are also heat sensitive (37), and therefore it may be that the exact level of cortex cross-linking is important for full heat resistance and dormancy. However, because of the other effects of the *dacB* mutation on cortex structure (decrease in L-Ala and δ-lactam), this cannot be stated with certainty. It is interesting to note that spores of both *dacB* and *spmA* strains have an increase in the ratio of spore protoplast volume to sporoplast (protoplast-plus-cortex) volume (37). Thus, it is this parameter (which can alter without changes in water content) which may be crucial for spore heat resistance. The ratio can be effected either by changes in peptidoglycan structure (*dacB*) or by as-yet-unknown mechanisms. The *spoVD* gene encodes a putative penicillin-binding protein (12, 16) which most likely plays a crucial role in cortex biosynthesis since strain AA108 (*spoVD*) could not produce mature endospores for cortex structural analysis.

It has been proposed that muramic acid δ-lactam residue formation could occur by either the action of an *N*-acetylmuramyl-L-alanine amidase followed by transacylation or by de-*N*-acetylation followed by transpeptidation (49), although until the present work, no enzyme activity associated with this function has been identified. The *cwlD* gene was identified as encoding a putative sporulation-specific peptidoglycan hydrolase with sequence homology to the major vegetative cell amidase of *B. subtilis* 168 (44). A mutation in *cwlD* led to endospores which were blocked at the stage of cortex hydrolysis during germination and were unable to outgrow and form colonies on agar plates. However, the colony-forming ability of the mutant could be partially rescued, even after heat treatment, by the addition of lysozyme added to exogenously hydrolyze the spore cortex to allow outgrowth. It was proposed that CwlD may have one of two roles, either as a germination-specific lytic enzyme (GSLE) which hydrolyzes the cortex during germination or as a cortex maturation enzyme which sets up the correct cortical structure during sporulation to be recognized by the GSLE (44).

Cortex muropeptide analysis (Fig. 1C) revealed an incredibly simple profile for the *cwlD* mutant (strain AA107). This astonishing result is due to the complete absence of muramic acid δ-lactam residues in the cortex. The fact that muramic acid δ-lactam synthesis occurs during the latter phase of sporulation after cortex biosynthesis (59) suggests that the function of CwlD may be to cleave the peptide side chains from nascent peptidoglycan acting as an amidase. CwlD may itself be involved in the lactamization reaction, or the reaction may require other components. It seems that CwlD cleaves side chains irrespective of whether they are cross-linked, since the cross-linking index per Dpm residue in strain AA107 (*cwlD*) is unaltered. When calculated per muramic acid residue, however, AA107 has cortex with approximately double the cross-linking of the parent, although this does not greatly affect heat resistance. Muropeptides X and Y (Table 3) from AA110 (*dacB*) both have cross-linked side chains but with only one of the L-Ala amino termini linked to a glycan moiety. These muropeptides may be evidence of the activity of CwlD, which may have cleaved the peptide side chain from one glycan backbone. Both of these muropeptides seem to be present in strain HR (Fig. 1A) but are only at high enough levels to enable purification in AA110. Peptidoglycan hydrolases often show functional redundancy, enzymes being able to compensate for each other in a given process (45). CwlD, however, is essential for muramic acid δ-lactam residue formation and thus has a highly specialized role.

It is remarkable that although AA107 (*cwlD*) spores are entirely missing the most distinguishing feature of the spore cortex, they are still apparently stable. This leads to the question as to what is the role of the muramic acid δ-lactam residues? A clue to the answer to this question lies in the germination phenotype of the AA107 (*cwlD*) spores. These spores are unable to geminate past the stage of cortex hydrolysis. Thus, the muramic acid δ-lactam residues, produced during sporulation by CwlD, may be present on the spore cortex primarily to be recognized as part of the substrate specificity of the GSLE which hydrolyzes the spore cortex during germination. In support of this, it is known that GSLEs from spores of both *B. megaterium* and *B. cereus* have a very high degree of substrate specificity, only hydrolyzing intact, in situ spore cortex peptidoglycan containing muramic acid δ-lactam residues (18, 32). Such a high-specificity requirement of the GSLE is understandable, since it is essential during germination for the cortex to be hydrolyzed to allow spore outgrowth. It is as important for the primordial cell wall (which does not have muramic acid δ-lactam residues) to remain relatively intact. If the primordial cell wall is breached, then the germinating

spore protoplast will have no constraining peptidoglycan layer, with tragic consequences for the cell.

Mutations in none of the other genes whose products which may have a role in cortex or primordial cell wall biosynthesis had a noticeable effect on the muropeptide profile. Because of the possible functional redundancy of these components, it may only be by the creation of multiple mutants that their combined roles can be elucidated. It is also unknown as to how the single L-alanine side chains on the cortex arise, although an L-Ala–D-Glu endopeptidase has been isolated from sporulated cultures of *Bacillus thuringiensis* which may fulfill this role (29). Alternatively, sequential cleavage of the pentapeptide side chain by the action of a DD-carboxypeptidase, D-Glu–*meso*-Dpm endopeptidase, and an LD-carboxypeptidase capable of hydrolyzing L-Ala–D-Glu could result in the L-Ala C terminus (24). In support of this, a sporulation-associated D-Glu–*meso*-Dpm endopeptidase has been identified in *B. sphaericus* and *B. subtilis* (23, 24).

The application of RP-HPLC technology to the study of spore cortex peptidoglycan has revealed the relatively simple nature of the cortex as compared with the peptidoglycan of many other species (22, 43). Hidden within this very simplicity is the key as to how this polymer is able to maintain the extreme dormancy of bacterial endospores. By the continued study of cortex structure during development, in defined mutants, and the comparison of cortices from different species, we plan to further define the important elements of the endospore cortex during differentiation.

ACKNOWLEDGMENTS

We thank Christine Buchanan, Patrick Piggot, Junichi Sekiguchi, and Jeff Errington for provision of strains, R. Marquardt for the gift of Cellosyl, and David Popham and Peter Setlow for strains and sharing their unpublished results.

This work has been supported by the Food Directorate of the BBSRC (A.A.), the Royal Society (S.J.F.), Jubiläumsfond der Österreichischen Nationalbank (PDMS grant 4840 to G.A.), the Fonds zur Förderung der wissenschaftlichen Forschung (MALDIMS grant 11183 to G.A.), the European Community (HCM grant ERB CHRX CT940425 to P.Z.), and the ARC Programme (United Kingdom-Austria travel fund).

REFERENCES

1. **Alderton, G., and N. S. Snell.** 1963. Base exchange and heat resistance in bacterial spores. Biochem. Biophys. Res. Commun. **10:**139–143.
2. **Allmaier, G., M. C. Rodriguez, and E. Pittenauer.** 1992. Optimization of sample deposition for plasma desorption mass spectrometry of peptidoglycan monomers. Rapid Commun. Mass Spectrom. **6:**284–288.
3. **Allmaier, G., and E. R. Schmid.** 1993. New mass spectrometric methods for peptidoglycan analysis, p. 23–30. *In* M. A. de Pedro, J.-V. Holtje, and W. Loffelhardt (ed.), Bacterial growth and lysis: metabolism and structure of the bacterial sacculus. Plenum Press, New York.
4. **Allmaier, G., A. Zenker, P. Zöllner, B. Pfanzagl, and W. Loffelhardt.** 1996. MALDI mass spectrometry of peptidoglycan oligomers after size exclusion chromatography and HPLC. *In* Proceedings of the 44th American Society of Mass Spectrometry Conference, in press.
5. **Anagnostopoulos, C., and J. Spizizen.** 1961. Requirements for transformation in *Bacillus subtilis*. J. Bacteriol. **81:**741–746.
6. **Buchanan, C. E., and A. Gustafson.** 1992. Mutagenesis and mapping of the gene for a sporulation-specific penicillin-binding protein in *Bacillus subtilis*. J. Bacteriol. **174:**5430–5435.
7. **Buchanan, C. E., and M.-L. Ling.** 1992. Isolation and sequence analysis of *dacB*, which encodes a sporulation-specific penicillin-binding protein in *Bacillus subtilis*. J. Bacteriol. **174:**1717–1725.
8. **Buchanan, C. E., and S. L. Neyman.** 1986. Correlation of penicillin-binding protein composition with different functions of two membranes in *Bacillus subtilis* forespores. J. Bacteriol. **165:**498–503.
9. **Cano, R. G., and M. K. Borucki.** 1995. Revival and identification of bacterial-spores in 25-million-year-old to 40-million-year-old Dominican amber. Science **268:**1060–1064.
10. **Cleveland, E. F., and C. Gilvarg.** 1975. Selective degradation of peptidoglycan from *Bacillus megaterium* spores during germination, p. 458–464. *In* P. Gerhardt, R. N. Costilow, and H. L. Sadoff (ed.), Spores VI. American Society for Microbiology, Washington, D.C.
11. **Crowther, J. S., and A. C. Baird-Parker.** 1983. The pathogenic and toxigenic spore-forming bacteria, p. 275–311. *In* A. Hurst, and G. W. Gould (ed.), The bacterial spore, vol. 2. Academic Press Ltd., London.
12. **Daniel, R. A., S. Drake, C. E. Buchanan, R. Scholle, and J. Errington.** 1994. The *Bacillus subtilis spoVD* gene encodes a mother-cell-specific penicillin-binding protein required for spore morphogenesis. J. Mol. Biol. **235:**209–220.
13. **De Jonge, B. L. M., Y. S. Chang, D. Gage, and A. Tomasz.** 1992. Peptidoglycan composition in heterogeneous Tn*551* mutants of a methicillin-resistant *Staphylococcus aureus* strain. J. Biol. Chem. **267:**11255–11259.
14. **Dougherty, T. J.** 1985. Analysis of *Neisseria gonorrhoeae* peptidoglycan by reverse-phase, high-pressure liquid chromatography. J. Bacteriol. **163:**69–74.
15. **Ellar, D. J.** 1978. Spore specific structures and their function. Symp. Soc. Gen. Microbiol. **28:**295–334.
16. **Errington, J.** 1993. *Bacillus subtilis* sporulation: regulation of gene expression and control of morphogenesis. Microbiol. Rev. **57:**1–33.
17. **Forrest, T. M., G. E. Wilson, Y. Pan, and J. Schaefer.** 1991. Characterization of cross-linking of cell walls of *Bacillus subtilis* by a combination of magic-angle spinning NMR and gas chromatography-mass spectrometry of both intact and hydrolysed ^{13}C- and ^{15}N-labelled cell-wall peptidoglycan. J. Biol. Chem. **266:**24485–24491.
18. **Foster, S. J., and K. Johnstone.** 1987. Purification and properties of a germination-specific cortex-lytic enzyme from spores of *Bacillus megaterium* KM. Biochem. J. **242:**573–579.
19. **Gally, D., and S. Cooper.** 1993. Peptidoglycan synthesis in *Salmonella typhimurium* 2616. J. Gen. Microbiol. **139:**1469–1476.
20. **Gerhardt, P., and R. E. Marquis.** 1989. Spore thermoresistance mechanisms, p. 43–63. *In* I. Smith, R. Slepecky, and P. Setlow (ed.), Regulation of procaryotic development. American Society for Microbiology, Washington, D.C.
21. **Gerhardt, P., and W. G. Murrell.** 1978. Basis and mechanisms of spore resistance, p. 18–20. *In* G. H. Chambliss and J. C. Vary (ed.), Spores VII. American Society for Microbiology, Washington, D.C.
22. **Glauner, B., and U. Schwarz.** 1983. The analysis of murein composition with high-pressure-liquid chromatography, p. 29–34. *In* R. Hackenbeck, J.-V. Holtje, and H. Labischinski (ed.), The target of penicillin. de Gruyter, Berlin.
23. **Guinand, M., G. Michel, and G. Balassa.** 1976. Lytic enzymes in sporulating *Bacillus subtilis*. Biochem. Biophys. Res. Commun. **68:**1287–1293.
24. **Guinand, M., M. J. Vacheron, G. Michel, and D. J. Tipper.** 1979. Location of peptidoglycan lytic enzymes in *Bacillus sphaericus*. J. Bacteriol. **138:**126–132.
25. **Imae, Y., and J. L. Strominger.** 1976. Relationship between cortex content and properties of *Bacillus sphaericus* spores. J. Bacteriol. **126:**907–913.
26. **Imae, Y., M. B. Strominger, and J. L. Strominger.** 1978. Conditional spore cortexless mutants of *Bacillus sphaericus*, p. 62–66. *In* G. H. Chambliss and J. C. Vary (ed.), Spores VII. American Society for Microbiology, Washington, D.C.
27. **Jayatissa, P. M., and A. H. Rose.** 1976. Role of wall phosphomannan in flocculation of *Saccharomyces cerevisiae*. J. Gen. Microbiol. **96:**165–174.
28. **Johnstone, K., and D. J. Ellar.** 1982. The role of cortex hydrolysis in the triggering of germination of *Bacillus megaterium* KM endospores. Biochim. Biophys. Acta **714:**185–191.
29. **Kingan, S. L., and J. C. Ensign.** 1968. Isolation and characterization of three autolytic enzymes associated with sporulation of *Bacillus thuringiensis* var. *thuringiensis*. J. Bacteriol. **96:**629–638.
30. **Kohlrausch, U., and J.-V. Holtje.** 1991. Analysis of murein and murein precursors during antibiotic-induced lysis of *Escherichia coli*. J. Bacteriol. **173:**3425–3431.
31. **Linnett, P. E., and D. J. Tipper.** 1976. Transcriptional control of peptidoglycan precursor synthesis during sporulation in *Bacillus sphaericus*. J. Bacteriol. **125:**565–574.
32. **Makino, S., N. Ito, T. Inoue, S. Miyata, and R. Moriyana.** 1994. A spore-lytic enzyme released from *Bacillus cereus* spores during germination. Microbiology **140:**1403–1410.
33. **Margot, P., C. A. H. Roten, and D. Karamata.** 1991. *N*-Acetyl muramoyl-L-alanine amidase assay based on specific radioactive labeling of muropeptide L-alanine: quantitation of the enzyme activity in the autolysin deficient *Bacillus subtilis* 168, *flaD* strain. Anal. Biochem. **198:**15–18.
34. **Marquis, R. E., and G. R. Bender.** 1990. Compact structure of cortical peptidoglycans from bacterial spores. Can. J. Microbiol. **36:**426–429.
35. **Martin, S. A., R. S. Rosenthal, and K. Biemann.** 1987. Fast atom bombardment mass spectrometry and tandem mass spectrometry of biologically active peptidoglycan monomers from *Neisseria gonorrhoeae*. J. Biol. Chem. **262:**7514–7522.
36. **Pandey, N. K., and A. I. Aronson.** 1979. Properties of the *Bacillus subtilis* spore coat. J. Bacteriol. **137:**1208–1218.
37. **Popham, D. L., B. Illades-Aguiar, and P. Setlow.** 1995. The *Bacillus subtilis dacB* gene, encoding penicillin-binding protein 5*, is part of a three-gene operon required for proper spore cortex synthesis and spore core dehydration. J. Bacteriol. **177:**4721–4729.
38. **Popham, D. L., and P. Setlow.** 1993. The cortical peptidoglycan from spores

of *Bacillus megaterium* and *Bacillus subtilis* is not highly cross-linked. J. Bacteriol. **175:**2767–2769.
39. **Popham, D. L., and P. Setlow.** 1993. Cloning, nucleotide sequence, and regulation of the *Bacillus subtilis pbpE* operon, which codes for penicillin-binding protein 4* and an apparent amino acid racemase. J. Bacteriol. **175:**2917–2925.
40. **Popham, D. L., and P. Setlow.** 1993. Cloning, nucleotide sequence, and regulation of the *Bacillus subtilis pbpF* gene, which codes for a putative class A high-molecular-weight penicillin-binding protein. J. Bacteriol. **175:**4870–4876.
41. **Popham, D. L., and P. Setlow.** 1994. Cloning, nucleotide sequence, mutagenesis, and mapping of the *Bacillus subtilis pbpD* gene, which codes for penicillin-binding protein 4. J. Bacteriol. **176:**7197–7205.
42. **Popham, D. L., and P. Setlow.** 1995. Cloning, nucleotide sequence, and mutagenesis of the *Bacillus subtilis ponA* operon, which codes for penicillin-binding protein (PBP) 1 and a PBP-related factor. J. Bacteriol. **177:**326–335.
43. **Quintela, J. C., E. Pittenauer, G. Allmaier, V. Aran, and M. A. de Pedro.** 1995. Structure of peptidoglycan from *Thermus thermophilus* HB8. J. Bacteriol. **177:**4947–4962.
44. **Sekiguchi, J., K. Akeo, H. Yamamoto, F. K. Khasanov, J. C. Alonso, and A. Kuroda.** 1995. Nucleotide sequence and regulation of a new putative cell wall hydrolase gene, *cwlD*, which affects germination in *Bacillus subtilis*. J. Bacteriol. **177:**5582–5589.
45. **Smith, T. J., and S. J. Foster.** 1995. Characterization of the involvement of two compensatory autolysins in mother cell lysis during sporulation of *Bacillus subtilis* 168. J. Bacteriol. **177:**3855–3862.
46. **Snowden, M. A., H. R. Perkins, A. W. Wyke, M. V. Hayes, and J. B. Ward.** 1989. Cross-linking and *O*-acetylation of newly synthesized peptidoglycan in *Staphylococcus aureus* H. J. Gen. Microbiol. **135:**3015–3022.
47. **Sowell, M. O., and C. E. Buchanan.** 1983. Changes in penicillin-binding proteins during sporulation of *Bacillus subtilis*. J. Bacteriol. **153:**1331–1337.
48. **Stewart, G. S. A. B., K. Johnston, E. Hagelberg, and D. J. Ellar.** 1981. Commitment of bacterial spores to germinate. Biochem. J. **198:**101–106.
49. **Tipper, D. J., and J. J. Gauthier.** 1972. Structure of the bacterial endospore, p. 3–12. *In* H. O. Halvorson, R. Hanson, and L. L. Campbell, Spores V. American Society for Microbiology, Washington, D.C.
50. **Tipper, D. J., and P. E. Linnett.** 1976. Distribution of peptidoglycan synthetase activities between sporangia and forespores in sporulating cells of *Bacillus sphaericus*. J. Bacteriol. **126:**213–221.
51. **Todd, J. A., E. J. Bone, and D. E. Ellar.** 1985. The sporulation-specific enzyme penicillin-binding protein 5a from *Bacillus subtilis* is a DD-carboxypeptidase *in vitro*. Biochem. J. **230:**825–828.
52. **Todd, J. A., E. J. Bone, P. J. Piggot, and D. J. Ellar.** 1983. Differential expression of penicillin-binding protein structural genes during *Bacillus subtilis* sporulation. FEMS Microbiol. Lett. **18:**197–202.
53. **Todd, J. A., A. N. Roberts, K. Johnstone, P. J. Piggot, G. Winter, and D. J. Ellar.** 1986. Reduced heat resistance of mutant spores after cloning and mutagenesis of the *Bacillus subtilis* gene encoding penicillin-binding protein 5. J. Bacteriol. **167:**257–264.
54. **Vorm, O., P. Roepstorff, and M. Mann.** 1994. Improved resolution and very high sensitivity in MALDI TOF of matrix surfaces made by fast evaporation. Anal. Chem. **66:**3281–3287.
55. **Warburg, R. J., C. E. Buchanan, K. Parent, and H. O. Halvorson.** 1986. A detailed study of *gerJ* mutants of *Bacillus subtilis*. J. Gen. Microbiol. **132:**2309–2319.
56. **Warth, A. D.** 1978. Molecular structure of the bacterial spore. Adv. Microb. Physiol. **17:**1–47.
57. **Warth, A. D., and J. L. Strominger.** 1969. Structure of bacterial spores: occurrence of the lactam of muramic acid. Proc. Natl. Acad. Sci. USA **64:**528–535.
58. **Warth, A. D., and J. L. Strominger.** 1972. Structure of the peptidoglycan from spores of *Bacillus subtilis*. Biochemistry **11:**1389–1396.
59. **Wickus, G. G., A. D. Warth, and J. L. Strominger.** 1972. Appearance of muramic lactam during cortex synthesis in sporulating culture of *Bacillus cereus* and *Bacillus megaterium*. J. Bacteriol. **111:**625–627.
60. **Wu, J.-J., R. Schuch, and P. J. Piggot.** 1992. Characterization of a *Bacillus subtilis* sporulation operon that includes genes for an RNA polymerase σ factor and for a putative DD-carboxypeptidase. J. Bacteriol. **174:**4885–4892.
61. **Yanouri, A., R. A. Richard, J. Errington, and C. E. Buchanan.** 1993. Cloning and sequencing of the cell division gene *pbpB*, which encodes penicillin-binding protein 2B in *Bacillus subtilis*. J. Bacteriol. **175:**7604–7616.
62. **Zhang, J., P. C. Fitz-James, and A. I. Aronson.** 1993. Cloning and characterization of a cluster of genes encoding polypeptides present in the insoluble fraction of the spore coat of *Bacillus subtilis*. J. Bacteriol. **175:**3757–3766.